Coherence Constraint on the Existence of Cosmic Defects

Jiun-Huei Proty Wu*
Department of Physics and Institute of Astrophysics, National Taiwan University
No.1 Sec.4 Roosevelt Road, Taipei 10617, Taiwan
(Dated: February 2, 2008)

We devise a measure $n(r)$ to quantify a robust feature in the coherent cosmic perturbations, namely the narrowness of the first peak in the power spectrum of the Cosmic Microwave Background (CMB) anisotropy. A maximum-likelihood analysis using the WMAP data shows that the power fraction of any defect models at the first peak is persistently less than 4.5% at the 68% confidence. Our approach and results are insensitive to the uncertainties in the theoretical predictions for defect models, and thus the most robust to date. We show that to convert these results into realistic constraints on theories such as inflation, string cosmology, and SUSY GUTs, a more robust study for the cosmic-string-induced CMB around the degree scale is required.

PACS numbers: 98.70.Vc, 98.80.Cq, 98.80.Es

arXiv:astro-ph/0501239v1 13 Jan 2005

A. Introduction: Cosmic defects have been an interesting subject for different reasons through different decades. They were first introduced around the 70's as an inevitable consequence of various theories such as the quantum field theory and the unification theory [1, 2]. Then motivated by the anisotropy in the Cosmic Microwave Background (CMB) observed by COBE in 1992 [3], they competed with inflation as the dominant mechanism for the formation of structures in the universe [4, 5, 6, 7, 8, 9]. They started losing this contest in the recent years when the flood of high-precision data showed great agreement with inflation (e.g., [10, 11]). Nevertheless, defects have been still playing a key role in testing some of the fundamental physics, especially those related to inflation and string cosmology. In general, for example, various defects may form as hybrid inflation ends [12]. In string theory, colliding branes can not only bring the brane inflation to the end but also potentially generate cosmic strings [13, 14]. In the Supersymmetric (SUSY) Grand Unified Theories (GUTs), which embed the standard model into the string theory, cosmic strings can also be formed at the end of hybrid inflation [15, 16]. Therefore, we can use observational data to place limits on the energy density of cosmic defects, so as to confine the energy scales of the associated physical mechanisms. In this paper, we will employ the CMB data for this purpose.

There are two main types of defects: global defects (Models I–IV in Tab. I) and local cosmic strings (Models V–VII). Their resulting CMB power spectra are shown in Fig. 1. The CMB power spectrum is defined as $C_\ell = \langle |a_{\ell m}|^2 \rangle$, where $a_{\ell m}$'s are the multipole-expansion coefficients of the CMB temperature anisotropy, and ℓ is the multipole number. By comparing these results side by side, we find that the results for the $O(4)$ textures (Model III) in Ref.[5] and [8] agree well at the 10% level for $\ell < 1000$. On the other hand, the uncertainty in the theoretical predictions for cosmic strings remains large. Models V[17] and VI[6] are both based on a toy model using filaments to mimic strings, while Model VII[9] uses string simulations extrapolated from a non-expanding universe. These predictions disagree not only in shape but also in amplitude. For example, although based on the same approach, the predicted C_ℓ of Model VI [6] is higher than that of Model V [17] by a factor of 4 and 16 at $\ell = 10$ and 700 respectively (for the same string linear energy density μ, where $C_\ell \propto \mu^2$; see Fig. 1). Depending on the velocity of the decay products of the long strings, the amplitude and the shape of C_ℓ may vary significantly [9] (see Model VII in Fig. 1). These theoretical uncertainties have been overlooked in most of the recent studies about the observational constraint on μ and other related model parameters (e.g., [16, 17, 18]), dramatically weakening the conclusions therein (e.g., $G\mu \leq 2 \times 10^{-7}$ at 99% confidence in Ref.[17, 18], which used WMAP and SDSS data). Note that work employing full string simulations in an expanding universe has also been pursued [4, 7, 19, 20, 21, 22, 23] but only for ℓ up to a few tens due to the numerical limitation [22]. This ℓ range is not suitable for us to investigate the observational first peak at $\ell \approx 220$ (see later), so we will not consider this model here. It is still worthy mentioning that the C_{10} in Ref.[22] is about 8 times higher than that in Ref.[17] for the same μ.

In face of the above uncertainties in the theoretical work, we devise a new strategy to constrain the energy level and thus the existence of defects. This strategy focuses on a robust feature of the coherent cosmic perturbations—the narrowness of the first peak in C_ℓ.

B. Quantifying the coherence: We first define $\mathcal{C}_\ell = \ell(\ell+1)C_\ell/2\pi$. If the apex of the first peak in $\mathcal{C}_\ell$ is located at $\ell_{\rm p}$ with the height $\mathcal{C}_{\rm p} \equiv \mathcal{C}(\ell_{\rm p})$, and the width of the peak at the height $r\mathcal{C}_{\rm p}$ $(0 < r \leq 1)$ is $\Delta\ell(r)$ (see Fig. 2), then the new measure is defined as

$$n(r) = \frac{\Delta\ell(r)}{\ell_{\rm p}}. \qquad (1)$$

As will be justified and explained later, the shape of the function $n(r)$ is determined by the nature of whether the

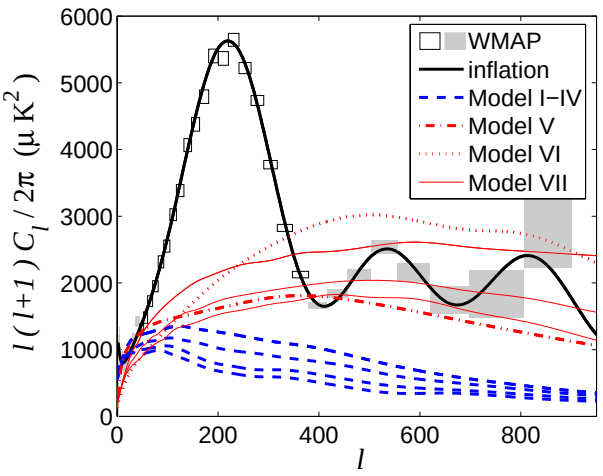

FIG. 1: CMB power spectra of global defects (blue dashed; Models I–IV downwards), local cosmic strings (red dot-dashed, red dotted, and red thin solid), the concordance model (black thick), and the WMAP (boxes; at 1-σ). The 19 empty boxes are used for the analysis of $n(r)$ and f^x_{220}. Model V is normalized with $G\mu = 2\times10^{-6}$; Models VI and VII are both with $G\mu = 7\times10^{-7}$ for the ease of comparison.

TABLE I: Cosmic defect models investigated here, and their power fraction f^x_{220} at $\ell = 220$, their temperature anisotropy $\sqrt{\mathcal{C}^x_\ell}$ at $\ell = 220$ and 10 (in μK), as constrained by WMAP, all at the 68% confidence.

x	Models	f^x_{220}	$\sqrt{\mathcal{C}^x_{220}}$	$\sqrt{\mathcal{C}^x_{10}}$	constraints
I	strings[5]	$\leq 4.5\%$	≤ 16	≤ 13	-
II	monopoles[5]	$\leq 4.4\%$	≤ 16	≤ 14	-
III	textures[5, 8]	$\leq 3.7\%$	≤ 14	≤ 15	$\epsilon \leq 8.2\times10^{-6}$
IV	$O(6)$ text.[5]	$\leq 3.0\%$	≤ 13	≤ 14	-
V	loc. cos. str.[17]	$\leq 3.4\%$	≤ 14	≤ 10	$G\mu \leq 7\times10^{-7}$
VI	loc. cos. str.[6]	$\leq 2.1\%$	≤ 11	≤ 4.6	$G\mu \leq 2\times10^{-7}$
VII	loc. cos. str.[9]	-	-	-	-

CMB perturbations are coherent or not. It depends only weakly on the geometry of the universe, because a change in geometry will stretch both $\Delta\ell$ and $\ell_{\rm p}$ in the same way, so that their ratio $n(r)$ remains very much unchanged.

To justify the robustness of this coherence feature in $n(r)$, we consider the inflationary models for a reasonably large region in the parameter space: $0 \leq \Omega_\Lambda \leq 1$ (energy density parameter for cosmological constant), $0.1 \leq \Omega_{\rm c} \leq 1$ (for cold dark matter), $0.01 \leq \Omega_{\rm b} \leq 0.2$ (for baryons), $0.5 \leq h \leq 0.9$ ($H_0 = 100h$ km s^{-1}Mpc^{-1} where H_0 is the Hubble parameter today), $0.8 \leq n_{\rm s} \leq 1.2$ (scalar spectral index), $0 \leq \tau \leq 0.25$ (optical depth). Note that this gives $0.11 \leq \Omega_{\rm t} \leq 2.2$ (total energy density parameter). First we compute all the CMB power spectra [24] within this parameter range, and then the resulting $n(r)$ for each spectrum. These $n(r)$'s occupy the blue shaded region in Fig. 3. It is clear that the coherence

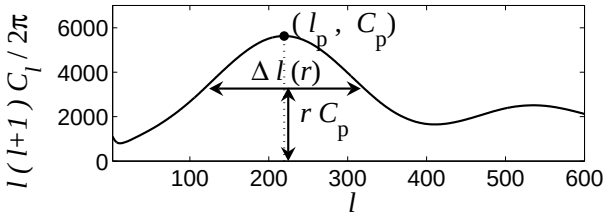

FIG. 2: Illustration for the definition of $n(r)$ in Eq. (1).

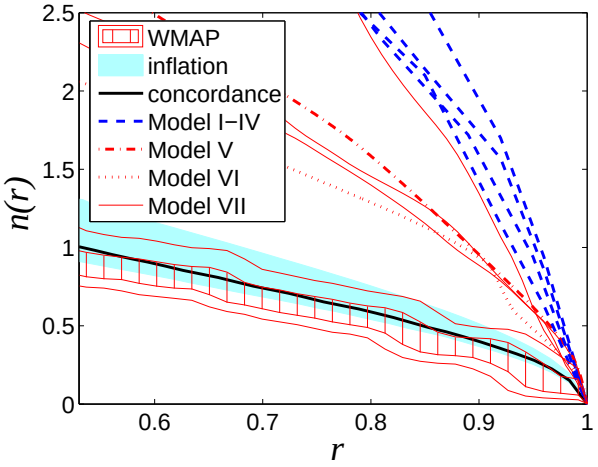

FIG. 3: The $n(r)$ of the concordance model and the defects (same line styles as in Fig. 1). Additionally, the inflationary models spam over the blue shaded region, and the red lined regions are the 68% and 95% C.R.'s from WMAP.

nature of the inflationary models confines the $n(r)$ within a very limited region on the r-n plane.

On the other hand, we compute the $n(r)$ for the defect models in Tab. I. Obviously the peaks in $\mathcal{C}_\ell$ for these incoherent models are much broader (Fig. 1), resulting in an $n(r)$ of at least twice higher at a given r (Fig. 3). A comparison between these lines and the shaded blue region shows the capability of $n(r)$ in discriminating the coherent and the incoherent models. This discrimination is independent of the cosmological parameters.

Theoretically this coherence feature in the $n(r)$ can be manifested by the following intuitive approach. In the synchronous gauge for a perturbation theory [21, 25], it is straight forward to show that with inflation the power spectrum of photon energy contrasts at the last-scattering epoch $\eta_{\rm ls}$ can be approximated by the form:

$$P(k) \propto k^{n_{\rm s}} \left[\frac{\cos\left(k\eta_{\rm ls}/\sqrt{3}\right)}{1+\left(k\eta_{\rm ls}\right)^2} e^{-(k\eta_D)^2}\right]^2, \qquad (2)$$

where k is the comoving wave number. The exponential term accounts for the photon-diffusion damping, with η_D typically one order below $\eta_{\rm ls}$ [26]. The cosine oscillations are due to the coherence nature of the perturbations, resulting from the fact that the inflationary perturba-

tions on the same scale (k^{-1}) entered the horizon at the same time ($\sim k^{-1}$) and thus oscillated coherently. On the other hand, for models with only defects, the perturbations on the same scale were seeded over a range of time after the horizon crossing, and thus oscillated incoherently. These incoherent oscillations effectively remove the cosine dependence in Eq. (2), leaving only a broad peak around the scale $\eta_{\rm ls}$. We then compute $C_\ell \propto \int P(k) j_\ell(k\eta_0) k^2 dk$, where η_0 is the comoving radius of the last-scattering sphere and j_ℓ is the spherical Bessel function. We find that the resulting $n(r)$ for the coherent case is slightly lower than the blue shaded region in Fig. 3, due to the omission of the Doppler effect and the Integrated Sachs-Wolfe effect. These two effects are sub-dominant in the first peak and thus in $n(r)$. It is important to note that the cosine dependence in $P(k)$ gives not only the periodic peaks in C_ℓ as commonly known, but also the narrowness of the first peak as we try to advocate here. On the other hand, the incoherent case leads to a much broader peak in C_ℓ, resulting in an $n(r)$ of at least twice larger than the coherent case.

The cosmic perturbations may be attributed to both coherent and incoherent mechanisms. Given the fact that the former is the dominant, an increasing fraction of the latter in a mix model will broaden the width of the first peak, resulting in a higher value of $n(r)$. In the following, we will invoke this feature to constrain the fraction of the incoherent perturbations and thus the defects.

C. Observational constraint: From observations, we can estimate $n(r)$. Among the large amount of CMB results that measure the first peak in $\mathcal{C}_\ell$, we choose the WMAP [27] because it is the most stringent to date. We will denote its result as $(\ell_{i(\rm l)}, \ell_{i(\rm r)}, \mathcal{C}_i, \sigma_i)$, where i indicates the i-th ℓ bin, $\ell_{i(\rm l)}$ and $\ell_{i(\rm r)}$ denote respectively the smallest and the largest ℓ within the bin, $\mathcal{C}_i$ is the binned power, and σ_i is the 1-σ error in $\mathcal{C}_i$. For a given point $A(\ell'_{\rm p}, \mathcal{C}'_{\rm p})$ on the ℓ-$\mathcal{C}_\ell$ plane, the probability that it is the apex of the first peak is

$$P_1(A) = pdf(\mathcal{C}'_{\rm p}; \mathcal{C}_a, \sigma_a) \prod_{i\neq a} cdf(\mathcal{C}'_{\rm p}; \mathcal{C}_i, \sigma_i), \qquad (3)$$

where a denotes the a-th ℓ bin within which $\ell'_{\rm p}$ lies (i.e. $\ell'_{\rm p} \in [\ell_{a(\rm l)}, \ell_{a(\rm r)}]$), $pdf(x;\mu,\sigma)$ is a normal probability distribution function with mean μ and standard deviation σ, $cdf(x;\mu,\sigma)$ is a normal cumulative probability distribution function. Then at the height $r\mathcal{C}'_{\rm p}$ ($0 < r \leq 1$), the probablility for point $B(\ell'_{\rm l}, r\mathcal{C}'_{\rm p})$ being the left-end point of the peak and $\Delta\ell'$ being the width of the peak is

$$\begin{aligned} P_2(B, \Delta\ell'|A) = & \prod_{\ell_{i(\rm r)}<\ell'_{\rm l} \text{ or } \ell'_{\rm l}+\Delta\ell'<\ell_{i(\rm l)}} cdf(r\mathcal{C}'_{\rm p}; \mathcal{C}_i, \sigma_i) \\ & \times \prod_{\ell'_{\rm l}<\ell_{i(\rm l)} \ \&\ \ell_{i(\rm r)}<\ell'_{\rm l}+\Delta\ell'} \left[1 - cdf(r\mathcal{C}'_{\rm p}; \mathcal{C}_i, \sigma_i)\right] \\ & \times I(\ell'_{\rm l}; r\mathcal{C}'_{\rm p}, \ell_{b(\rm l)}, \ell_{b(\rm r)}) I(\ell'_{\rm l}+\Delta\ell'; r\mathcal{C}'_{\rm p}, \ell_{c(\rm r)}, \ell_{c(\rm l)}), \end{aligned} \qquad (4)$$

where b and c denote respectively the ℓ bins within which the $\ell'_{\rm l}$ and the $\ell'_{\rm l}+\Delta\ell'$ are, and $I(x; r\mathcal{C}'_{\rm p}, \ell_{i(1)}, \ell_{i(2)})$ is a linear-interpolation function between $(\ell_{i(1)}, 1 - cdf(r\mathcal{C}'_{\rm p}; \mathcal{C}_i, \sigma_i))$ and $(\ell_{i(2)}, cdf(r\mathcal{C}'_{\rm p}; \mathcal{C}_i, \sigma_i))$ according to x. Here the condition $\ell'_{\rm l} < \ell'_{\rm p} < \ell'_{\rm l} + \Delta\ell'$ is also imposed. Finally, given the observational data, the probability for a point on the r-n plane to be present is

$$P(r,n) = \sum_{A, \Delta\ell'/\ell'_{\rm p}=n} P_1(A) P_2(B, \Delta\ell'|A). \qquad (5)$$

For each r, we compute the 68% and the 95% confidence regions (C.R.) for n, as shown in Fig. 3. Note that for the WMAP data, we use only the 19 bins (i = 12–30; $45 \leq \ell \leq 379$) that best confine the first peak. These bins are shown as the empty boxes in Fig. 1.

It is quite clear in Fig. 3 that the observational data strongly favor the inflationary models, regardless of the geometry of the universe. Thus a defect-dominated universe with a very closed geometry, which serves to shift the first peak from several hundreds to around 220, is totally inconsistent with the observations. Also plotted in Fig. 3 is the $n(r)$ of the concordance model based on the data of WMAP, CBI, ACBAR, 2dF, Ly-alpha [11]. Its power spectrum is shown in Fig. 1. Its $n(r)$ is roughly within the 68% C.R. of the data. We also note from Fig. 3 that on average the data favor a slightly narrower peak than what is predicted by the inflationary models.

To see how stringent the observed narrowness of the first peak can constrain the existence of cosmic defects, we further consider the following mixed power spectrum:

$$\mathcal{C}_\ell^{\rm tot} = A\left[f_{220}^x \frac{\mathcal{C}_{220}^{\rm inf}}{\mathcal{C}_{220}^x}\mathcal{C}_\ell^x + (1-f_{220}^x)\mathcal{C}_\ell^{\rm inf}\right], x = \text{I–VI}, \qquad (6)$$

where the superscripts 'inf' and 'x' denote the contribution from inflation and from the defect models in Tab. I respectively. Model VII is not considered here because Ref.[9] does not provide information about the dependence of the $\mathcal{C}_\ell$ on the cosmological parameters. Here f_{220}^x is nothing but the power fraction of the defects at the first peak ($\ell_{\rm p} \approx 220$), and A is an arbitrary normalization factor. We use the WMAP data to constrain f_{220}^x, again using only the 19 ℓ bins. A standard maximum-likelihood analysis is performed for the parameters of f_{220}^x, A, Ω_Λ, $\Omega_{\rm c}$, $\Omega_{\rm b}$, h, $n_{\rm s}$, τ, with the flat-geometry constraint that $\Omega_{\rm t} = \Omega_\Lambda + \Omega_{\rm c} + \Omega_{\rm b} = 1$. We then marginalize over all the parameters except for f_{220}^x, leaving only a one-dimensional likelihood $\mathcal{L}(f_{220}^x)$. At the 68% confidence level (C.L.), the estimated values of f_{220}^x are shown in Tab. I. Two robust features in all results for different models are that the likelihood $\mathcal{L}(f_{220}^x)$ peaks below $f_{220}^x = 1.2\%$, and that $f_{220}^x \leq 4.5\%$ (or equivalently $\sqrt{\mathcal{C}_{220}^x} \leq 16\mu$K) at the 68% C.L. This means that the defect models contribute at most 4.5%, preferably below 1.2%, in the observed $\mathcal{C}_{220}$, or equivalently that their contribution to the CMB anisotropy around the degree

scale is no more than 16μK, preferably below 8.2μK. The $\sqrt{\mathcal{C}_{10}^x}$ in Tab. I is extrapolated from the value of $\sqrt{\mathcal{C}_{220}^x}$ taking the corresponding model shape of $\mathcal{C}_\ell^x$. We see that $\sqrt{\mathcal{C}_{10}^x} \leq 15\mu$K (around the COBE scale) for all models.

D. Discussion and Conclusion: We emphasize that although the shape and the amplitude of $\mathcal{C}_\ell^x$ vary a lot among different defect models, the observational constraint on their f_{220}^x remains persistently below 4.5%. When we replace the $\mathcal{C}_\ell^x$ in Eq. (6) with a $\mathcal{C}_\ell$ which has $d\mathcal{C}_\ell/d\ell = m$, the same conclusion persists for $-10 \leq m \leq 10$. This indicates that any further improvement on the detailed predictions of $\mathcal{C}_\ell^x$ for defect models can only marginally affect our results here. In theory this is naturally due to the fact that the predicted $\mathcal{C}_\ell^x$'s are lack of curvature around the observational first peak at $\ell \approx 220$, so that a larger f_{220}^x will result in a higher $n(r)$, which potentially violates the observational data.

Our results can be converted to place limits on the parameters in various theories. For example, the result $\sqrt{\mathcal{C}_{10}^{\rm III}} \leq 15\mu$K can be converted to $\epsilon = 4\pi G\phi_0^2 \leq 8\times10^{-6}$, leading to a constraint on the energy level of symmetry breaking $\phi_0 \leq 9.9\times10^{15}$GeV. This is consistent with, though more conservative than, the result in Ref.[28], where the full WMAP data were used to yield $f_{10}^{\rm III} \leq 13\%$, or equivalently $\sqrt{\mathcal{C}_{10}^{\rm III}} \leq 10\mu$K, at 95% C.L.

For local cosmic strings, naively we can take the more conservative result for μ, from Model V (see Tab. I), to yield a constraint on the symmetry-breaking scale $\eta \sim \mu^{1/2} \leq 10^{16}$GeV. In the context of string theory, where the strings are D-branes, it places an upper limit onto the superstring scale $M_{\rm s} \approx (\mu/2)^{1/2} \leq 7\times10^{15}$GeV. In the context of SUSY GUTs, a combination of our further deduced result $Q_{rms-PS}^V \equiv (\delta T)_Q^V \leq 4.4\mu$K and the study in Ref.[16] yields an upper limit on the mass scale of the F-term inflation $M \leq 2\times10^{15}$GeV, and on the superpotential coupling $\kappa \leq 2\times10^{-5}$. For the D-term inflation, we get constraint on the gauge coupling $g \leq 1.4\times10^{-2}$, and on the superpotential coupling $\lambda \leq 2.2\times10^{-5}$. We emphasize that all these constraints still carry considerable uncertainties due to the large uncertainties in the predicted $\mathcal{C}_{220}$ for strings, as addressed in the introduction. This uncertainty is propagated into the constraint on μ and thus on the deduced parameters. This is readily seen by the inconsistency between $G\mu \leq 7\times10^{-7}$ and 2×10^{-7} for Models V and VI respectively (see Tab. I). Therefore a more robust predictions for strings around the degree scale will dramatically settle this uncertainty. For the same reason, whether or not the values of $G\mu = 5.9\times10^{-7}$ [29] and 4×10^{-7} [30] that were required to explain the recent anomalous observations in the gravitational lens systems is consistent with the current CMB constraint remains an open question. Nevertheless, we are confident that $\sqrt{\mathcal{C}_{220}^{\rm str}} \leq 14\mu$K.

In conclusion, we invoke a coherence feature—the narrowness of the first peak in $\mathcal{C}_\ell$—to constrain the existence of defects. We show that the power fraction of any defect models at the first peak is persistently less than 4.5% at the 68% C.L., in spite of the large uncertainties in the current theoretical study (see Tab. I for the more detailed results). Hence our results should be the most objective and thus the most robust to date.

We acknowledge the support from the National Science Council of Taiwan (NSC 92-2112-M-002-047; NSC 93-2112-M-002-015).

* jhpw@phys.ntu.edu.tw; http://jhpw.phys.ntu.edu.tw

[1] G. t'Hooft, Nucl. Phys. B **79**, 276 (1974).
[2] T. W. B. Kibble, J. Phys. A **9**, 1387 (1976).
[3] G. F. Smoot *et al.*, Astroph. J. Lett. **396** (1992).
[4] B. Allen, R. R. Caldwell, E. P. S. Shellard, A. Stebbins, and S. Veeraraghavan, Phys. Rev. Lett. **77**, 3061 (1996).
[5] U. L. Pen, U. Seljak, and N. Turok, Phys. Rev. Lett. **79**, 1611 (1997).
[6] A. Albrecht, R. A. Battye, and J. Robinson, Phys. Rev. Lett. **79**, 4736 (1997).
[7] P. P. Avelino, E. P. S. Shellard, J. H. P. Wu, and B. Allen, Phys. Rev. Lett. **81**, 2008 (1998).
[8] R. Durrer, M. Kunz, and A. Melchiorri, Phys. Rev. D **59**, 123005 (1999).
[9] C. Contaldi, M. Hindmarsh, and J. Magueijo, Phys. Rev. Lett. **82**, 679 (1999).
[10] A. H. Jaffe *et al.*, Phys. Rev. Lett. **86**, 3475 (2001).
[11] D. N. Spergel *et al.*, Astroph. J. Suppl. Ser. **148**, 175 (2003).
[12] E. J. Copeland *et al.*, Phys. Rev. D **49**, 6410 (1994).
[13] S. Sarangi and S.-H. H. Tye, Phys. Lett. B **536**, 185 (2002).
[14] G. Dvali and A. Vilenkin, JCAP **403**, 10 (2004).
[15] R. Jeannerot, J. Rocher, and M. Sakellariadou, Phys. Rev. D **68**, 103514 (2003).
[16] J. Rocher and M. Sakellariadou, hep-ph/0406120; hep-ph/0412143 (accepted by Phys. Rev. Lett.) (2004).
[17] L. Pogosian *et al.*, Phys. Rev. D **68**, 23506 (2003).
[18] L. Pogosian, M. Wyman, and I. Wasserman, JCAP **9**, 8 (2004).
[19] F. R. Bouchet, D. P. Bennett, and A. Stebbins, Nature **335**, 410 (1988).
[20] J. H. P. Wu, P. P. Avelino, E. P. S. Shellard, and B. Allen, Int. J. Mod. Phys. D **11**, 61 (2002).
[21] J. H. P. Wu, Ph.D. thesis, University of Cambridge, available at http://jhpw.phys.ntu.edu.tw (1999).
[22] M. Landriau and E. P. S. Shellard, Phys. Rev. D **69**, 023003 (2004).
[23] J. H. P. Wu, Mod. Phys. Lett. A **19**, 1019 (2004).
[24] U. Seljak and M. Zaldarriaga, Astroph. J. **469**, 437 (1996).
[25] A. Albrecht *et al.*, Phys. Rev. Lett. **76**, 1413 (1996).
[26] W. Hu and N. Sugiyama, Astroph. J. **471**, 542 (1996).
[27] G. Hinshaw *et al.*, Astroph. J. Suppl. Ser. **148**, 135 (2003).
[28] N. Bevis, M. Hindmarsh, and M. Kunz, Phys. Rev. D **70**, 043508 (2004).
[29] M. Sazhin *et al.*, Mon. Not. R. Astron. Soc. **343**, 353 (2003).
[30] R. Schild *et al.*, Astron. Astrophys. **422**, 477 (2004).